# Geochemical characteristics of soil gas radon and tectonic implications to the Anninghe and Zemuhe faults in Sichuan, Southwestern of China

2018 IEF Annual Meeting

YING LI [1*], ZHI CHEN [1], YAO YANG [2], FENGXIA SUN [1]

*E-mail: subduction6@hotmail.com

[1] CEA Key Laboratory of Earthquake Forecasting (Institute of Earthquake Forecasting), China Earthquake Administration, Beijing 100036, China

[2] Sichuan Earthquake Agency, Chengdu 610041, China

## 1 Introduction

The spatio-temporal variations of soil gas Rn at an active fault zone may reflect the regional crustal stress/strain changes related to seismo-tectonic activity (Yang et al., 2006; Fu et al., 2008; Zhou et al., 2010; Koike at al., 2014). The Anninghe fault (ANHF) and the Zemuhe fault (ZMHF) located along the eastern boundary of the Sichuan-Yunnan block (southwestern of China), are some of the most active faults. These faults mainly control the seismicity of southwestern area of China. Rn concentrations in soil gas are measured across the ANHF and the ZMHF. The geochemical characteristic of Rn in these areas is determined and its correlation to the activity of fault is discussed by geostatistics of the Rn data attained at 394 sampling points along 15 profiles. In addition, the tectonic activity of the ANHF and the ZMHF is evaluated used relative Rn activity of faults ($K_Q$) suggested by Seminsky and Bobrov (2009) and Seminsky and Demberel (2013).

## 2 Seismogeological settings and sampling sites

Our study areas are located in the intersection of the ANHF and the ZMHF on the southeastern margins of the Tibetan Plateau (Fig. 1a). The ANHF and the ZMHF systems show characteristics of a left-lateral strike-slip movement since late Quaternary (Xu et al., 2003a,b) and control the main seismic activity in southwest China (Wen et al., 2008). For the first time, we carried out a cross-sectional soil gas Rn measurement along 15 profiles at Yangfushan in the southern segment of the ANHF (site 1, 3 profiles), Dajingliangzi in the northern segment of the ZMHF (site 3, 3 profiles) and Xiaomiao Township, the intersection part of them (site 2, 9 profiles)(Fig. 1b-c), respectively. Totally, 394 sampling points were measured for soil gas Rn concentration.

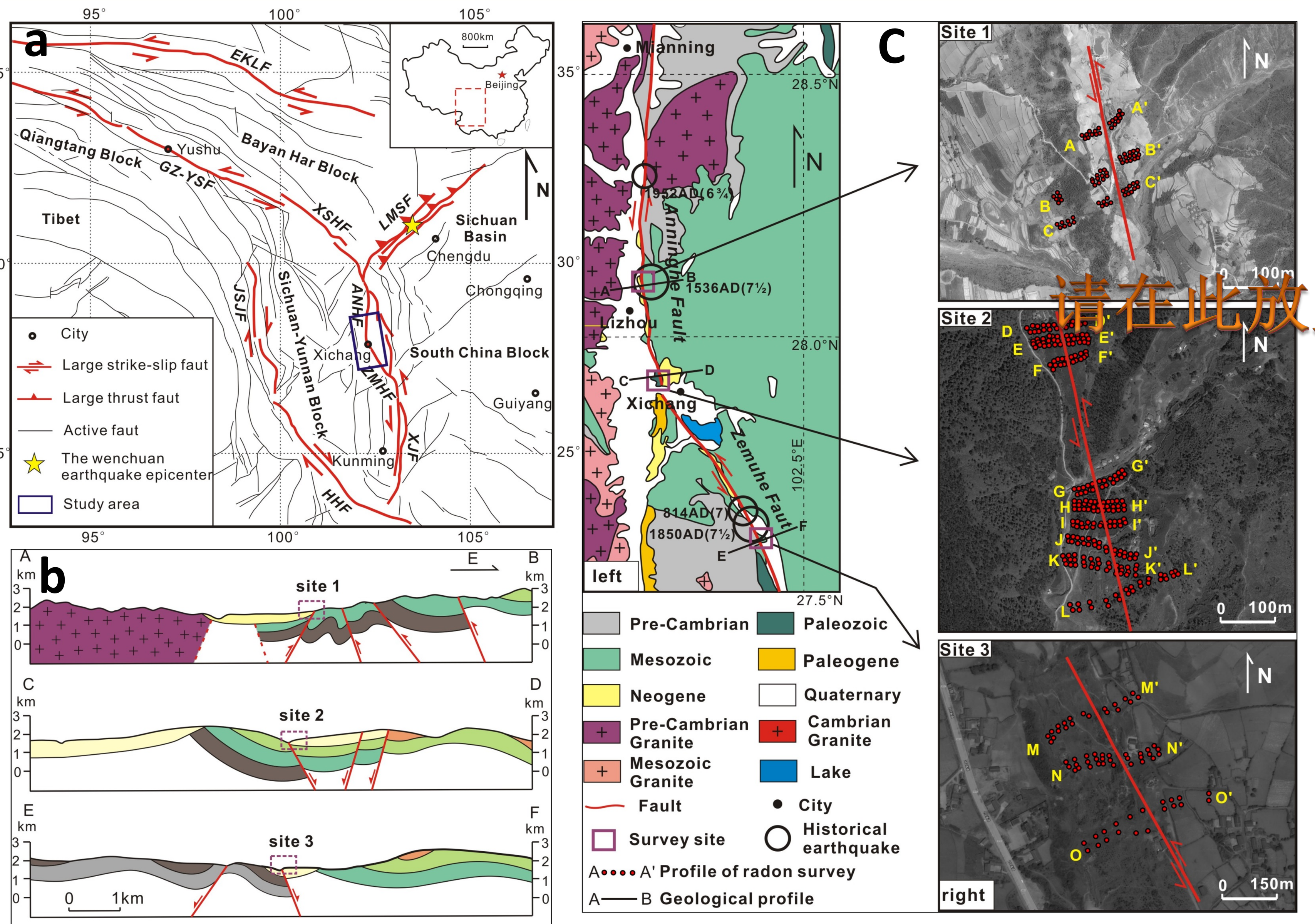

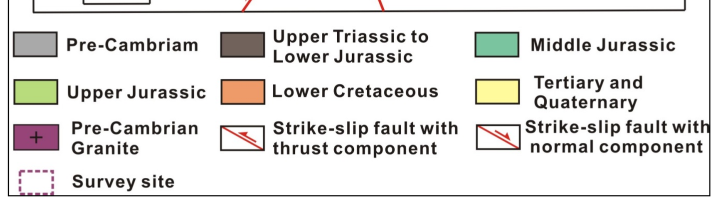


Fig. 1 (a)-Tectonic map of the eastern Tibetan Plateau and the study area (modified after Wang et al., 2013); (b)-Geological profiles of the survey sites (modified after Seismological Bureau of Sichuan Province, 2013a,b); (c)-Geological map of study area (left) (modified after Ren et al., 2010, 2014) and plot map of the points of the soil gas Rn sampled along the ANHF and the ZMHF (right)

## 3 Soil gas survey

Soil gas Rn was sampled by inserting a hollow stainless steel sampler into the ground at a depth of 80 cm. Rn survey was carried out in the field using a RAD 7 Rn detector (Durridge COMPANY Inc., Bedford, USA) which counts the α particles emitted during the decay of $^{222}Rn$ to $^{218}Po$ for the counting of Rn concentration (Fig. 2). The sensitivity and measurement error of Rn detector are 14.8 $Bq/m^3$ and ±5%, respectively.

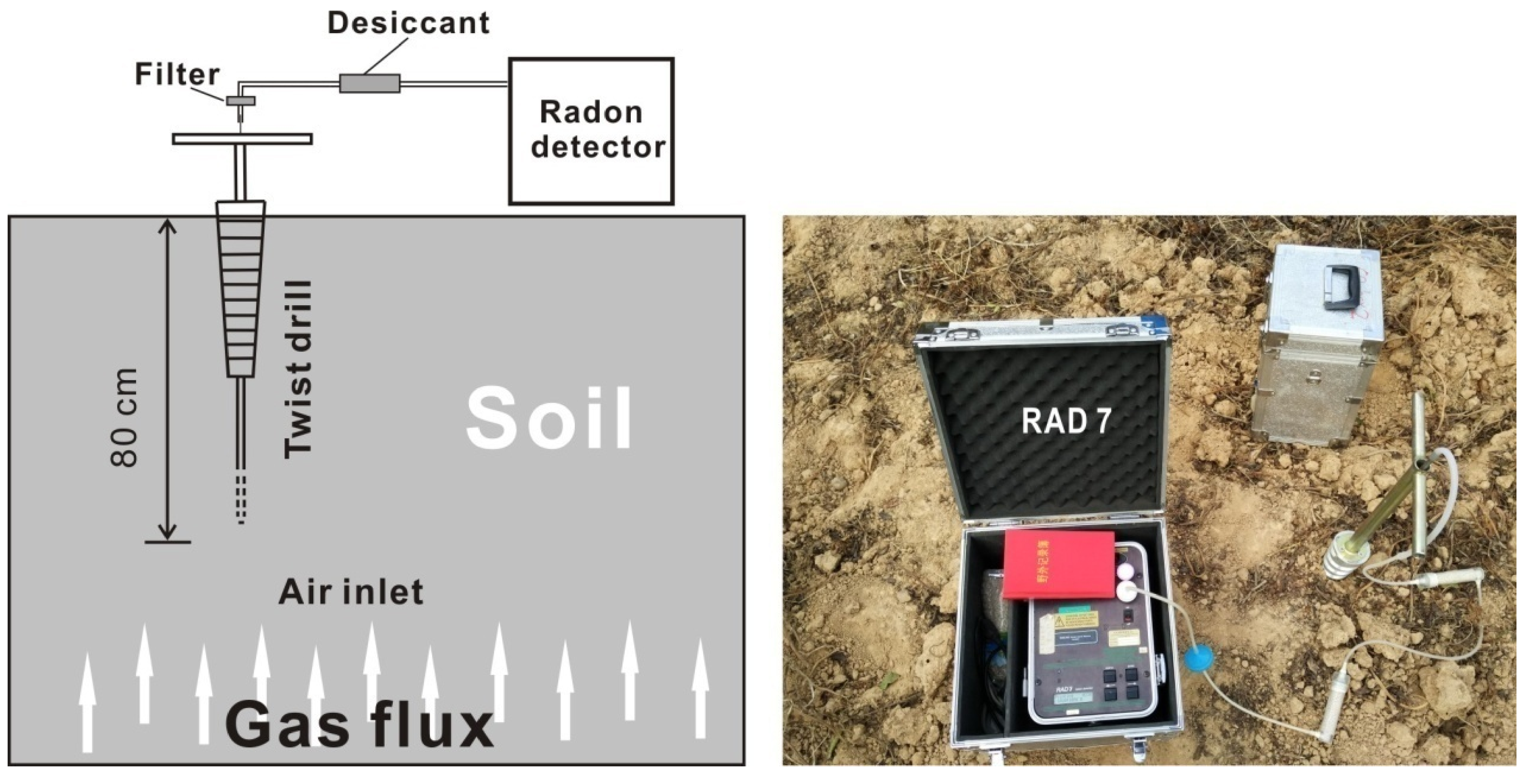


Fig. 2 Sampling scheme and instrument employed for soil gas Rn concentration measurement.

## 4 Results

Statistics of the Rn concentrations attained in the study area are listed in Table 1. Seminsky and Bobrov (2009) and Seminsky and Demberel (2013) used relative Rn activity of faults ($K_Q$), to evaluate the fault activity by soil gas emission, which is the ratio of maximum concentration ($Q_{max}$), to minimum concentration ($Q_{min}$) in any fault wall for a fault next to the fault-related anomaly. To calculate this index, we use either an average of two values of $Q_{min}$, determined for each wall of the fault, or one values of $Q_{min}$, if the damage zone is not completely cut by the profile (e.g., Fig. 3, profile A-A') In the curves, the value of each point is determined by the mean value of the Rn concentrations attained in the 2 or 3 parallel survey lines in the specific position of the profile). The faults can be classified by contrast of the associated soil gas Rn concentration anomalies into three groups with high ($K_Q$>6), medium (6>$K_Q$>3) and low ($K_Q$<3) activity. As can be seen from Fig. 4

**Table 1. Soil Gas Statistics of the study area**

| Number of site | Name of profile/m | Length of profile/ m | Mean /($Bq/m^3$) | Minimum /($Bq/m^3$) | Maximum, $Q_{max}$ /($Bq/m^3$) | $Q_{min}$ /($Bq/m^3$) | SD /($Bq/m^3$) | Skewness /($Bq/m^3$) | H/m | $K_Q$ |
|---|---|---|---|---|---|---|---|---|---|---|
| 1 | A-A' | 135 | 18866 | 6842 | 42200 | 6842 | 13216 | 0.94 | 52 | 6.2 |
| | B-B' | 150 | 18283 | 6114 | 31202 | 9568 | 10280 | 0.06 | 70 | 3.3 |
| | C-C' | 165 | 27550 | 4595 | 77650 | 8495 | 23121 | 1.03 | 75 | 9.1 |
| 2 | D-D' | 150 | 7999 | 2373 | 13986 | 3522 | 4124 | 0.11 | 55 | 4.0 |
| | E-E' | 165 | 6931 | 2314 | 11060 | 2314 | 3248 | -0.09 | 83 | 4.8 |
| | F-F' | 135 | 4402 | 1703 | 10400 | 1703 | 3029 | 1.36 | 28 | 6.1 |
| | G-G' | 165 | 8856 | 3721 | 17728 | 5395 | 3812 | 0.97 | 36 | 3.3 |
| | H-H' | 135 | 10239 | 3435 | 15461 | 3435 | 3580 | -0.66 | 88 | 4.5 |
| | I-I' | 165 | 9766 | 2420 | 19109 | 3650 | 6018 | 0.46 | 86 | 5.2 |
| | J-J' | 165 | 9035 | 1837 | 16061 | 1837 | 4492 | 0.06 | 95 | 8.7 |
| | K-K' | 162 | 10194 | 5305 | 18329 | 6458 | 4803 | 0.85 | 74 | 2.8 |
| | L-L' | 180 | 7673 | 2871 | 15922 | 2871 | 4176 | 1.08 | 30 | 5.5 |
| 3 | M-M' | 135 | 11417 | 7495 | 15883 | 7495 | 3169 | 0.41 | 34 | 2.1 |
| | N-N' | 135 | 14366 | 8273 | 20119 | 8273 | 4095 | 0.18 | 53 | 2.4 |
| | O-O' | 135 | 14666 | 6219 | 22433 | 8832 | 5951 | 0.08 | 45 | 2.5 |

Maximum/ $Q_{max}$ - maximum value of the Rn concentrations in soil gas; Minimum - minimum value of the Rn concentrations in soil gas; $Q_{min}$ - minimum value of the Rn concentrations in soil gas just outside the fault anomaly (*-counted as average value on estimations in both fault wings); H - width of Rn anomalous domain; $K_Q$ - index of soil gas Rn activity.



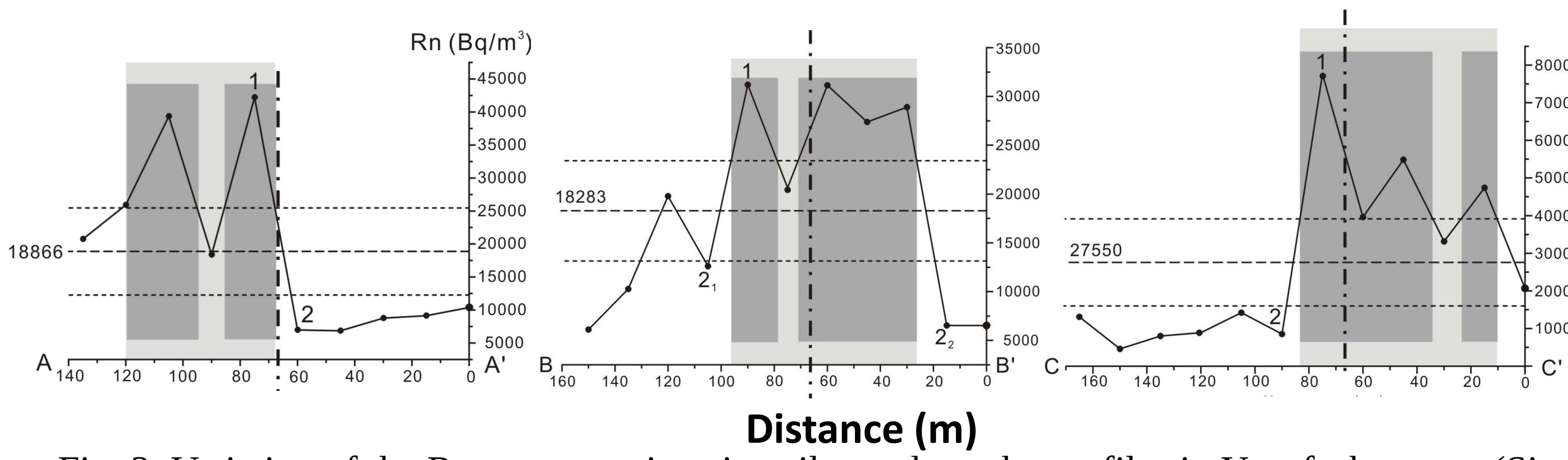


Fig. 3. Variation of the Rn concentrations in soil gas along the profiles in Yangfushan area (Site 1). 1–Profile number; 2–curve of variation of the Rn concentrations (Q) along the profiles; 3–position of fault in curves; 4–mean ($Q_{mean}$) of soil gas Rn; 5–levels of $Q_{mean}$ ± $^1/_2$SD (SD=standard deviation); 6–value of soil gas Rn concentration, representing major maximums in the fault-related anomaly and minimum(s) next to the fault-related anomaly; 7–profile domains with anomalous Rn concentrations in soil gas (Q>$Q_{mean}$+$^1/_2$SD); 8–soil gas Rn fault-related anomaly associated with fault.

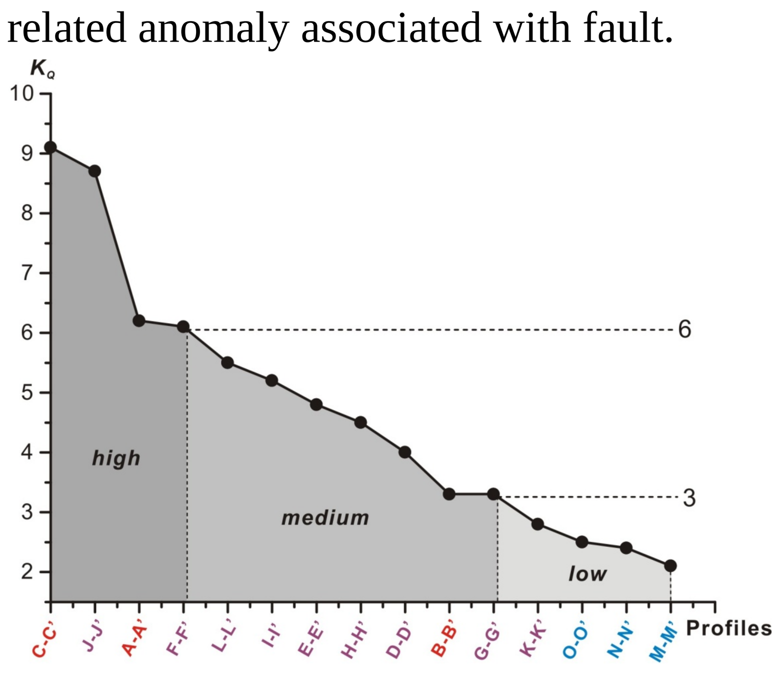


Fig. 4. Curve for comparison of soil gas Rn anomalies revealed in study area in terms of contrast, $K_Q$ values of the profiles (Table 1) are shown in the curve in the order of decreasing. The several profiles in site 1 are marked with red, in site 2 are purple and in site 3 are sky-blue.

## 5 Conclusion

1. The Rn concentrations in soil gas have been measured across the ANHF and the ZMHF for the first time. The background and maximum value of the Rn concentrations in the southern segment of the ANHF are significantly higher than that of the northern segment of the ZMHF. It indicates that the faults with high slip rate are more favorable for discharging gas from the deep.
2. The relative index $K_Q$ of the Rn activity of the southern segment of the ANHF is obviously higher than that of the northern segment of the ZMHF. It indicates that tectonic activity of the south segment of the ANHF is stronger than that of the north segment of the ZMHF. The tectonic activity level of the intersection part of the ANHF and the ZMHF is in the median of them.